PHYSICAL REVIEW B VOLUME 47, NUMBER 1 1 JANUARY 1993-I

Superconductor–Mott-insulator transition in Bose systems with finite-range interactions

C. Bruder
Institut für Theoretische Festkörperphysik, Universität Karlsruhe, 7500 Karlsruhe, Federal Republic of Germany

Rosario Fazio
Istituto di Fisica, Università di Catania, viale A. Doria 6, 95128 Catania, Italy
and Institute for Theoretical Physics, University of California, Santa Barbara, California 93106

Gerd Schön
Institut für Theoretische Festkörperphysik, Universität Karlsruhe, 7500 Karlsruhe, Federal Republic of Germany
and Institute for Theoretical Physics, University of California, Santa Barbara, California 93106
(Received 26 May 1992)

We study the superconductor-insulator transition of Bose-Hubbard models with finite-range interactions. Commensurability of the charge distribution with the underlying lattice leads to a richly structured phase diagram. In addition to the lobes of insulating phase characterized by integer fillings, we find—for finite-range interactions—lobes with rational filling factors. At low temperatures we can investigate the phase transition by mapping the model onto a XXZ spin-$\frac{1}{2}$ Heisenberg model.

I. INTRODUCTION

Two-dimensional Bose-Hubbard models have been studied as models for superconducting films and arrays of Josephson junctions.[1–5] At low temperatures and with increasing strength of the hopping matrix element t they show a transition from an insulating to a superconducting phase. The chemical potential μ controls the number of bosons $\langle n \rangle$ per site. The resulting low-temperature phase diagram in the t-μ plane consists of a series of lobes. Inside the lobes (i.e., for t small compared to the Coulomb interaction energy) the system is insulating; outside it is superconducting. Apart from an overall scale factor, proportional to $1/\langle n \rangle$, the lobe structure depends periodically on μ.

In most of the previous work on this problem only on-site Coulomb repulsion U_0 has been considered. In this limit the lobes are centered around integer values of μ/U_0. Each lobe is characterized by an integer number of bosons per site—the same for each site—and a correspondingly defined compressibility vanishes.[1–3] In real systems the interaction has a finite range. In this case a much more structured phase diagram emerges.[5] We find further lobes with rational filling factors. In these lobes the charges form a superlattice that is commensurate with the underlying lattice.

In this paper we will exploit the analogies of Bose-Hubbard models and quantum-spin models to further support these conclusions and to derive further quantitative results. Away from the centers of the main lobes at $\mu \propto$ *integer* we can map the Bose-Hubbard model onto a spin-$\frac{1}{2}$ XXZ Heisenberg model. Different phases of the magnetic model correspond to different commensurate charge lattices, which are insulating, or to (different) superconducting phases. For instance, if we take on-site and nearest-neighbor Coulomb interactions into account, denoted by U_0 and U_1, respectively, we find two different types of lobes, one with integer filling, the other with half-integer filling, alternating with increasing μ. The width of the half-integer lobe (in the μ direction) is proportional to $U_1/(U_0+4U_1)$, and it extends to the symmetry (Heisenberg) point $t \propto U_1$. Longer-range interactions lead to further lobes with more general rational fillings. It can also lead to different superconducting states (supersolids).[6,7]

In one dimension the spin-$\frac{1}{2}$ XXZ Heisenberg model has been studied in much detail.[8–12] Using these results we can determine the critical properties of the one (1D) Bose-Hubbard model. Further results can be obtained in a large-S mean-field approximation and from the spin-wave analysis. Finally we can solve the full quantum problem for small clusters. The different approaches give us a rather complete picture of the phase transition.

II. THE EQUIVALENT MODELS

The Bose-Hubbard model with a finite range of the interaction can be written as

$$H = -\frac{1}{2}t \sum_{<ij>} b_i^\dagger b_j + \text{H.c.} + \frac{1}{2}\sum_{i,j} U_{ij} n_i n_j - \mu \sum_i n_i. \tag{1}$$

Here b_i is a Bose annihilation operator, and $n_i = b_i^\dagger b_i$ is the number of bosons at site i, which is controlled by the chemical potential μ. The hopping-matrix element is denoted by t. The interaction term is written in a form that is nonzero already for a single boson per site. We could remove this contribution by subtracting a term $(1/2)\sum_i U_{ii}n_i$, which merely corresponds to a shift in the chemical potential. The combination of interaction and chemical potential term depend periodically on

$$\hat{\mu} = \frac{\mu}{\sum_i U_{0i}} \tag{2}$$

with period 1. However, the hopping term is still sensitive to the value of n_i. As a result the phase diagram is not strictly periodic. It becomes so approximately at large particle numbers.

The Bose-Hubbard model is similar to the quantum phase model of arrays of mesoscopic Josephson junctions.[13,5] In small capacitance junctions we have to take into account the interaction between the charges Q_i on the islands. Most important are the capacitances C_1 associated with the junctions themselves and the capacitances C_0 of the islands with respect to a common ground. (Second-nearest-neighbor capacitances are usually of the same order as C_0 and can be ignored for the present purposes.) The charges interact with the inverse capacitance matrix C_{ij}^{-1}, which has a finite range. It decays exponentially for distances exceeding $\lambda = \sqrt{C_1/C_0}$. If a voltage V_x is applied to the array relative to the common ground (to be distinguished from a transport voltage) the energy provided by the voltage source $V_x \sum_i Q_i$ has to be included in the Hamiltonian. Obviously V_x takes the role of a chemical potential in the Bose-Hubbard model. The voltage-dependent term can be rewritten in terms of the "charge frustration" $Q_x = V_x/\sum_i C_{0i}^{-1} = C_0 V_x$. If we ignore quasiparticle tunneling, which will be discussed further below, we have $Q_i = 2en_i$, and the Hamiltonian of the array is

$$H = \frac{1}{2}\sum_{i,j}(Q_i - Q_x)C_{ij}^{-1}(Q_j - Q_x) - \sum_{<ij>} E_J \cos(\phi_i - \phi_j) \tag{3}$$

with

$$Q_i = \frac{\hbar}{i}\frac{\partial}{\partial(\hbar\phi_i/2e)} .$$

In contrast to the Bose-Hubbard model the properties of the quantum phase model (3) are strictly periodic in V_x. Both models are equivalent in the limit of large particle numbers per site, provided that we identify the Josephson coupling with the product of the particle number and the hopping term $E_J = \langle n_i + 1\rangle t$.[1,5]

We assume now that the reduced chemical potential $\hat{\mu}$ (or $Q_x/2e$) lies between two integers, not too close to either one

$$n < \hat{\mu} < n + 1. \tag{4}$$

Then for strong on-site interaction $U_{ii} \equiv U_0 \gg t,\, k_B T$ the particle number per site takes only one of the two integer values n or $n+1$ bracketing $\hat{\mu}$. This means we have to consider only two states per site, and the Bose-Hubbard model (and the quantum phase model for the Josephson-junction array) can be replaced by a spin-$\frac{1}{2}$ Heisenberg model[14]

$$H = \frac{1}{2}\sum_{i,j} U_{ij} S_i^z S_j^z - J \sum_{<ij>} [S_i^x S_j^x + S_i^y S_j^y] - h \sum_i S_i^z . \tag{5}$$

The spin operators $S_i^z = n_i - n - \frac{1}{2}$ replace the particle number n_i (or $Q_i/2e$), while the rising and lowering operators $S_i^{\pm} = S_i^x \pm iS_i^y$ replace the creation and annihilation operators $b_i^\dagger$ and b_i [or $\exp(\pm i\phi_i)$], respectively. If the reduced chemical potential is exactly half integer $\hat{\mu} = n + \frac{1}{2}$ the two states with $n_i = n$ and $n_i = n+1$ bosons per site are degenerate. Otherwise this symmetry is broken, which introduces a field term

$$h = (\hat{\mu} - n - \tfrac{1}{2})\sum_i U_{0i} . \tag{6}$$

The effect of the hopping term depends on the particle number. In the interval given by Eq. (4) the coupling strength in xy direction is

$$J = (n+1)t . \tag{7}$$

The reduction to a spin problem becomes exact for hard-core bosons $U_0 = \infty$. Of course, in this case the (quasi)periodic dependence on the chemical potential is not observable. However, the additional lobes, which we will discuss in the following, corresponding to fractional filling, also emerge for this case.

III. NEAREST-NEIGHBOR INTERACTION

We first assume that the interaction U_{ij} is restricted to on site and nearest neighbors only, and denote it by $U_{ii} = U_0$, $U_{ij} = U_1$ for i and j nearest neighbors (z nearest neighbors), and $U_{ij} = 0$ otherwise. Then the model (5) reduces to a spin-$\frac{1}{2}$ XXZ Heisenberg model with nearest-neighbor coupling. The on-site energy U_0 sets the scale for the chemical potential; it has to be retained in the definition of h. Longer-range interactions, which introduce longer-range couplings of the z components of the spins, will be discussed below. In the spin model the coupling in z direction is antiferromagnetic, that in xy direction is ferromagnetic. In bipartite lattices we can rotate the spins of one sublattice by π around the z axis, thus making the coupling antiferromagnetic also in xy direction. In this rotated form some of the symmetries are more obvious, but for definiteness we will use in the following the original spin variables, i.e., those explicit in Eq. (5).

Several qualitative and quantitative properties of the Bose-Hubbard model can be deduced at this stage. On the symmetry axis $h = 0$, i.e. $\hat{\mu} = n + \frac{1}{2}$, the ground state of the model (5) in dimensions $D \geq 2$ is a Néel state in the z direction for strong U_1 or a ferromagnetic state in the xy plane for strong J. They are separated by a phase transition at the symmetry (Heisenberg) point

$$(J/U_1)_{\rm cr} = 1 \quad \text{for } h = 0. \tag{8}$$

(This property can easily be understood in terms of the rotated spins. In this case both states are Néel states, oriented in the z direction or in the xy plane, depending on the relative strength of U_1 and J.) The Néel state oriented in the z direction corresponds to a superlattice of the bosons (a Wigner lattice, but commensurate with the underlying lattice). Apart from a uniform background of n bosons per site the expectation value of the boson number $\langle n_i \rangle$ alternates from site to site, forming a checkerboard pattern. The average density is $n+\frac{1}{2}$. This state is a Mott insulator. The particle-hole symmetry of the problem implies that the total number of bosons is constant in this phase, independent of the chemical potential. Hence, the compressibility $\kappa \propto \partial\langle\sum_i n_i\rangle/\partial\mu$ vanishes. The ferromagnetic state in the xy direction is characterized by long-range order of the operators $S_i^{\pm}$. Since they replace the operators $b_i^{\dagger}$ and b_i [or the functions $\exp(\pm i\phi_i)$ of the phases of the junction array] this state is superconducting.

Off the symmetry axis, $h \neq 0$, the field term weakens the Néel state, which reduces the critical value of J/U_1. The ferromagnetic state in the xy direction is favored. It is canted, however, to acquire a component in field direction. The average number of bosons $\langle\sum_i n_i\rangle$ changes continuously as a function of $\hat{\mu}$, which implies a finite compressibility. Finally, for strong fields the system goes into a paramagnetic state with magnetization pointing into the field direction. This state has the same number of bosons on each site (n or $n+1$, depending on the sign of h) and is insulating again. The results obtained so far are shown in Fig. 1. The Néel states, which arise as a consequence of the finite-range interaction, produce lobes in the phase diagram centered at half-integer values of $\hat{\mu}$. The paramagnetic states are what is left in our approach of the lobes centered around integer values. These integer lobes also exist in a model with on-site interactions only.[1]

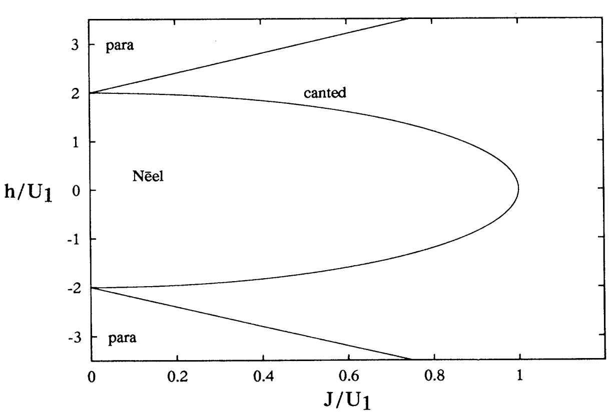

FIG. 1. The classical phase-diagram of a two-dimensional Bose-Hubbard model with nearest-neighbor interaction U_1. The field h of the spin problem is related to the chemical potential of the Bose model by $h = \mu - (n+1/2)(U_0+4U_1)$. The "half-integer" lobe in the center corresponds to a Néel state, which means the bosons form a superlattice with n and $n+1$ bosons on every other site. The paramagnetic phase at the bottom (top) marks the onset of the lobe with integer filling by n $(n+1)$ bosons on every site.

They shrink in the presence of finite-range interactions.

Further rigorous conclusions can be drawn and the critical exponents can be determined if we consider a one-dimensional chain. We first study the problem on the symmetry line $h = 0$. The Jordan-Wigner representation for the spins $S = \frac{1}{2}$ can be employed, which introduces a Fermi field, to map the problem onto a Luttinger model.[8,9] The bosonized version of the Luttinger model can be reformulated as a sine-Gordon field theory with the action

$$S[\Phi] = \int dx d\tau \left\{ \tfrac{1}{2}\chi\left[(\partial_\tau\Phi)^2 + (\partial_x\Phi)^2\right] + g\cos(2\Phi)\right\}. \tag{9}$$

At this stage the coefficients are undetermined. However, from the Bethe-ansatz solution one knows[10] that

$$\chi = \frac{1}{2\pi}\left(1 - \frac{1}{\pi}\cos^{-1}\frac{U_1}{J}\right).$$

The action has been studied in Refs. 8, 9, and 12. The model shows a phase transition of the Kosterlitz-Thouless (KT) type at a critical value $U_1 = J$. In the (massive) disordered phase the correlation length diverges as $\xi \propto \exp[-a(1-J/U_1)^{-1/2}]$, where a is some constant. The ordered phase is massless with a power-law decay of the correlation functions. The disordered and ordered phases correspond to Néel order in the z direction and to ferromagnetic order in the xy direction, respectively, which in turn correspond to the insulating and superconducting phases of the Bose-Hubbard model.

Off the symmetry axis, i.e., for $h \neq 0$, the sine-Gordon field theory acquires the term[11]

$$-\frac{h}{2\pi}\int dx\, d\tau\, \partial_x\Phi\ . \tag{10}$$

This action has been studied as a model for the commensurate-incommensurate transition.[12,15,16] For small fields the disordered phase remains the Néel state, but the critical value of J/U_1 is shifted. More interesting, the transition is changed into a second-order transition. On the ordered (superconducting) side the critical exponents for the correlation length and the specific heat and the dynamical exponent are $\nu = \frac{1}{2}, \alpha = \frac{1}{2}$, and $z = 2$, respectively. They coincide with the mean-field values. Approaching the transition from the disordered side (the Néel state) the specific heat does not diverge.[15]

It is interesting to compare the properties derived here for the half-integer lobe with those derived by Fisher *et al.*[1] and Batrouni and co-workers[2] for the integer lobe of the model with on-site interaction only. In 1D the transition is a KT transition in the maxima of both types of lobes, and it is a second-order transition elsewhere. In both cases the critical exponents take mean-field values if one approaches the phase transition from the ordered side.

Further quantitative results, and results for general dimensions can be obtained from the large S expansion. (In the following we concentrate on $D = 2$.) In this limit we compare the energies of different spin configurations assuming that the spins are classical vectors. As long as the interaction is restricted to nearest-neighbor couplings (U_1), only the three states mentioned above need to be considered.

(i) The Néel state oriented in the z direction with spins $\pm\frac{1}{2}$ on the two sublattices, corresponding to an insulating superlattice of n or $n+1$ bosons per site, is realized for small fields $|h| \leq h_0$, where

$$h_0 = 2\sqrt{U_1^2 - J^2} \; . \tag{11}$$

The phase boundary takes a lobelike shape.

(ii) For larger fields the spins are ferromagnetically ordered in the xy direction but canted in the z direction. The angle relative to the z axis is given by $2\langle S_i^z \rangle = \cos(\alpha) = (1/2)h/(U_1 + J)$. This state is superconducting, with a continuous change of the expectation value of the number of bosons as a function of μ.

(iii) For strong fields $|h| \geq h_1$, where

$$h_1 = 2(U_1 + J) \; , \tag{12}$$

a transition to the paramagnetic state occurs where all spins point in the z direction, corresponding to a uniform distribution of bosons. At $J = 0$ a direct transition occurs between the Néel state and the paramagnetic state.

In the magnetic problem the critical value of the field h_1 separating the canted state from the paramagnetic state is linear in J. Applied to the Bose-Hubbard model, where $h = \hat{\mu} - n - \frac{1}{2}$, this result ceases to be correct when $\hat{\mu}$ approaches an integer, say n. In this case the state with n bosons per site dominates and those with $n-1$ and $n+1$ become degenerate. Hence our restriction to a two-state problem becomes insufficient. The correct phase boundary between the superconducting and the insulating state with integer number of bosons per site also takes a lobelike shape.[1]

The classical phase diagram can be complemented by the usual spin-wave analysis. Applied to the Néel state we find the following spectrum of the excitations:

$$\omega(\mathbf{k}) = -|h| + 2\sqrt{U_1^2 - J^2\gamma(\mathbf{k})} \; , \tag{13}$$

where $\gamma(\mathbf{k}) = [\cos(k_x) + \cos(k_y)]/2$. The Néel state is stable within the phase boundaries obtained classically. On the other hand, the staggered magnetization is reduced by quantum fluctuations from $+\frac{1}{2}$ per site to

$$\frac{1}{2} - \frac{1}{2N}\sum_{\mathbf{k}}\left(\frac{U_1}{\sqrt{U_1^2 - J^2\gamma^2(\mathbf{k})}} - 1\right) . \tag{14}$$

Applied to the Bose model this means that for finite hopping amplitude J the expectation value of the excess number of bosons per site deviates from the classical values n or $n+1$. However, the average value does not change, which implies that the compressibility remains zero within this lobe. A similar analysis of the paramagnetic state shows that it too is stable within the classical phase boundary. In this case the magnetization is not reduced by quantum fluctuations, which means the number of bosons is precisely n or $n+1$ in the two phases. It is interesting that the spin model reproduces this result, which follows from the particle-hole symmetry of the Bose-Hubbard model.

We can also solve the full quantum problem if we restrict ourselves to small clusters. For a 2×2 cluster with periodic boundary conditions this can be done analytically. The total spin in the z direction is a good quantum number, which immediately allows a partial diagonalization. For small fields h and weak J the ground state is a superposition of the two Néel-like states oriented in the z direction with a small mixing ($\propto J$) of the remaining states with zero magnetization. For larger J, of the order of U_1, the ground state changes continuously into a state mixing all the basis states with zero total magnetization. Above a critical field $h_0 = U_1 - 2J + \sqrt{U_1^2 + 8J^2}$ another state, a superposition of the states with magnetization 1, has the lowest energy. At still larger fields, above the critical field h_1 given by Eq. (12), the paramagnetic state with maximum polarization in field direction becomes favorable. For small J the transitions obtained from the quantum cluster model agree well with the result of the large-S expansion. However, in the small cluster we do not find the transition at small h at a critical value of J/U_1. An improvement of the analysis requires either considering larger clusters, which is beyond the scope of the present paper, or else to embed the small cluster in a staggered mean field.

IV. FINITE-RANGE INTERACTIONS

We now consider longer-range interactions. In this case the phase diagram acquires further structure. We had studied this problem within the so-called "coarse graining" approach in Ref. 5, and found a rather complex phase diagram with different phases corresponding to various rational filling factors. We can reproduce these results within the large-S expansion presented above. For definiteness we assume here that the interaction is characterized by on-site, nearest-neighbor and second-nearest-neighbor interactions, $U_0 > U_1 > U_2$. In this case further spin configurations need to be considered. In addition to the states already discussed we find a ferrimagnetic phase corresponding to $\frac{1}{4}$ and $\frac{3}{4}$ filling in which the spins arrange in a 2×2 unit cell with three spins pointing in the field direction and one opposite. This corresponds to one excess (or deficit) boson on every fourth site. These phases lead to additional lobes in the phase diagram, which are shown in Fig. 2.

We also find more general superconducting states. For finite J, the Néel state and the $\frac{1}{4}$-lobe state are separated by two phases, viz., the "$\alpha - \beta$" state with a 2×2 unit cell characterized by two canting angles, α and β, on the two diagonal sublattices, and the "$\alpha - \beta \pm \gamma$" state with canting angles α on one diagonal and $\beta \pm \gamma$ on the other. These phases have both long-range order in the xy direction, which implies superconductivity, and staggered magnetization in z direction, which implies a superlattice of the bosons. The coexistence of both types of order has been denoted as "supersolid."[6] (In Ref. 6 only spin configurations characterized by two sublattices were considered. Consequently the $\frac{1}{4}$ lobe and the "$\alpha - \beta \pm \gamma$"

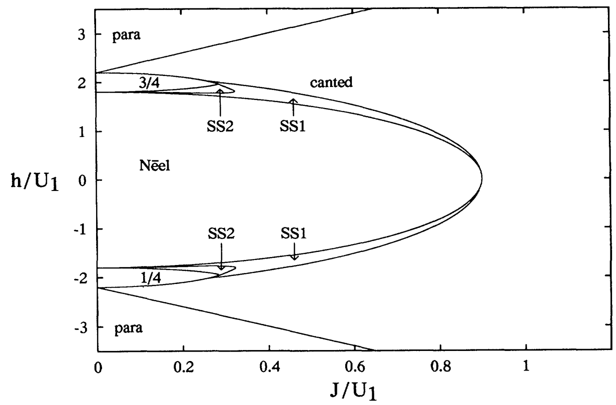

FIG. 2. Same as in Fig. 1, but second-nearest-neighbor interactions are included as well. We assume $U_2 = 0.1U_1$. Shown are the insulating lobes with filling factors (modulo 1) 0, $\frac{1}{4}$ (same as $\frac{3}{4}$), and $\frac{1}{2}$. In addition, we find different supersolid phases SS1 and SS2, which are characterized by two angles ("$\alpha - \beta$" phase) or three angles ("$\alpha - \beta \pm \gamma$") in a 2×2 unit cell.

state had not been noticed.)

Most of the phase boundaries can be determined analytically. They are for the boundaries between the paramagnetic and the canted state: $h_1 = 2(U_1 + U_2 + J)$, the canted state and the $\frac{1}{4}$ lobe: $h = U_1 + U_2 + J + \sqrt{(U_1 + U_2 + J)(U_1 + U_2 - 3J)}$, the canted and the "$\alpha - \beta$" state: $h = 2(U_1 + U_2 + J)\sqrt{(U_1 - U_2 - J)/(U_1 - U_2 + J)}$, and the "$\alpha - \beta$" and the Néel state: $h_0 = 2\sqrt{(U_1 - U_2)^2 - J^2}$. The boundary between the $\frac{1}{4}$ lobe and the "$\alpha - \beta \pm \gamma$" state is given by

$$J^2 = U_1^2 - U_2^2 - [\, h^3 - 2(2U_1 + U_2)h^2 + 4(U_1^2 + 2U_1U_2 - U_2^2)]/(8U_2)\,.$$

At this stage—for an interaction that is truncated beyond U_2—the $\frac{1}{4}$ lobe appears to have properties very similar to the other lobes discussed above. The spin-wave analysis shows that the excitation spectrum has a gap within the phase boundary obtained from the classical analysis. Furthermore, since the total spin $\sum_i S_i^z$ is conserved, the compressibility in this lobe should vanish as in the other lobes. However, there exist also important differences between the $\frac{1}{4}$ lobe and the half-integer and integer lobes. The former does not have the particle-hole symmetry of the latter two. The differences become apparent, when we consider longer-range interactions.

Longer-range interactions lead to more complicated insulating states with higher-order rational fillings. For instance, a phase with $\frac{1}{3}$ filling appears when we include U_3. These additional states with higher rational filling are not separated from each other or from the $\frac{1}{4}$ lobe by a superconducting phase reaching to $J = 0$. Instead they are separated by first-order transitions. For small J the critical value of h separating them follows from consideration of the Coulomb interaction only. On the classical level the transition line is independent of J. Lowest-order quantum corrections in J renormalize the interaction[17] and bend the transition lines. However, they do not change the nature of the transition. Therefore, we also expect that the fractionally filled states are incompressible and insulating.

In the absence of screening the interactions have an infinite range. This limit is realized in a junction array if the self-capacitance is very small $C_0 \ll C_1$.[18,17,5] In two dimensions the charges interact with a logarithmic dependence on the distance, similar as the vortices interact. A duality exists between charges and vortices, which allows us to draw conclusions about the phase diagram in the limit of long-range interactions. It is known that the magnetic frustration f leads to a phase diagram, which as a function of f looks like the wing of Hofstadter's butterfly.[19,20] In view of the duality, we expect a similar dependence of the phase diagram on the chemical potential or charge frustration. Even in this long-range limit the interaction decays with increasing distance. In particular we have $U_1/U_0 < \frac{1}{4}$. The opposite case appears unrealistic to us. However, it was considered in Ref. 21 and was shown to lead to an instability, namely, that two particles on one site are preferred to a uniform charge distribution.

V. DISCUSSION

It is well known that for the case of an on-site interaction the phase diagram of the Bose-Hubbard model shows a series of lobes of the Mott-insulating phase characterized by an integer number of particles per site. If we consider a more general interaction allowing nearest-neighbor interaction, U_1, we obtain secondary lobes separating the integer lobes. The new lobes correspond to the "checkerboard" Wigner lattice of excess bosons with expectation values in the window $n \leq \langle n_i \rangle \leq n + 1$, which alternate from site to site. If we continue to longer-range interactions further lobes appear. They correspond to higher commensurate phases in which a fraction of the lattice sites is occupied in a periodic fashion. Here we discussed the effect of U_2, which leads to a $\frac{1}{4}$ lobe. Taking into account longer-range interactions leads to an ever more complicated picture. However, the integer and half-integer lobes remain well defined with the properties described above. Similar conclusion have been reached recently in a different approach by Feigel'man and Ziegler.[22]

We now turn to the question of whether the lobe structure in the phase diagram can be observed in a realistic Josephson-junction array. This would require that disorder, for instance arising from charged impurities, does not play a role, and that the quasiparticles are completely frozen out. Even if the disorder is weak, the effect of quasiparticle tunneling on the ground-state properties is actually never negligible. In good quality tunnel junctions the subgap quasiparticle current can be extremely small, so small that it cannot be detected in an I-V characteristic. However, at any finite temperature the rate for inelastic scattering of electrons is finite (in contrast to the rate for creation and recombination of particle-hole pairs it vanishes only like a power of T). These inelastic processes smear out the density of states and lead to a nonvanishing quasiparticle current. (An estimate for dirty Al at $T = 10$ mK yields a current that is 8–10 orders of magnitude smaller than the normal-state current).

This means that the ground-state charge configuration is determined by quasiparticle tunneling. Single-electron charges interact with the same finite-range inverse capacitance matrix as Cooper-pair charges. Hence, we will find, for weak Josephson tunneling, a sequence of insulating phases, characterized by commensurate lattices formed by single electron charges. As a result the periodic dependence on the applied voltage is half that what we expect for pure Cooper-pair tunneling. Stronger Josephson tunneling leads to a transition into a superconducting state. The details of the phase boundary depend on the interplay between Cooper pair and single electron tunneling. If we can assume that the single-electron charges remain frozen (in the configuration they assume in the absence of Cooper-pair tunneling), we still have to generalize the procedure outlined above such as to consider a site-dependent charge frustration (and hence site-dependent field h_i). The results will differ in many details from what we described above. However, the periodic dependence of the phase diagram on the applied voltage still should be observable.

It would also be interesting to study normal tunnel junction arrays. There one also observes a transition between an insulating and a conducting phase at low temperatures.[18,17] Also this transition depends in a periodic fashion on an applied voltage. We can mention that a periodic dependence on gate voltages is seen routinely in systems consisting of a small number of tunnel junctions.

ACKNOWLEDGMENTS

We would like to acknowledge stimulating and helpful discussion with I. Affleck, A. Kampf, S. Sachdev, and G. Zimanyi. The research is part of the Sonderforschungsbereich 195 supported by the Deutsche Forschungsgemeinschaft. The research is also supported by the National Science Foundation under Grant No. PHY89-04035.

[1] M.P.A. Fisher, B.P. Weichman, G. Grinstein, and D.S. Fisher, Phys. Rev. B **40**, 546 (1989).

[2] G.G. Batrouni, R.T. Scalettar, and G.T. Zimanyi, Phys. Rev. Lett. **65**, 1765 (1990); R.T. Scalettar, G.G. Batrouni, and G.T. Zimanyi, *ibid.* **66**, 3144 (1991).

[3] M.P.A. Fisher, G. Grinstein, and S.M. Girvin, Phys. Rev. Lett. **64**, 587 (1990); M.-C. Cha, M.P.A. Fisher, S.M. Girvin, M. Wallin, and A.P. Young, Phys. Rev. B **44**, 6883 (1991).

[4] W. Krauth and N. Trivedi, Europhys. Lett. **14**, 627 (1991).

[5] C. Bruder, R. Fazio, A. Kampf, A. van Otterlo, and G. Schön, Phys. Scr. **42**, 159 (1992).

[6] H. Matsuda and T. Tsuneto, Suppl. Prog. Theor. Phys. **46**, 411 (1970); K.-S. Liu and M.E. Fisher, J. Low Temp. Phys. **10**, 655 (1972).

[7] A. Kampf and G. Zimanyi (private communication).

[8] M.P.M. den Nijs, Phys. Rev. B **23**, 6111 (1981).

[9] C.A. Doty and D.S. Fisher, Phys. Rev. B **45**, 2167 (1992).

[10] R. Baxter, Ann. Phys. (N.Y.) **70**, 193 (1972).

[11] H. Schulz, Phys. Rev. B **34**, 6372 (1986).

[12] M. Kardar, Phys. Rev. B **33**, 3125 (1986).

[13] For a number of articles see *Proceedings of the NATO Advanced Research Workshop on Coherence in Superconducting Networks, Delft, 1987*, edited by J.E. Mooij and G. Schön [Physica B **152** (1988)].

[14] T. Matsubara and H. Matsuda, Progr. Theor. Phys. (Kyoto) **16**, 569 (1956); M.E. Fisher, Rep. Prog. Phys. **30** 615 (1967).

[15] H. Schulz, Phys. Rev. B **22**, 5274 (1980).

[16] F.D.M. Haldane, P. Bak, and T. Bohr, Rev. B **28**, 2743 (1983).

[17] R. Fazio and G. Schön, Phys. Rev. B **43**, 5307 (1991); R. Fazio, A. van Otterlo, G. Schön, H.S.J. van der Zant, and J.E. Mooij, Helv. Phys. Acta **65**, 228 (1992).

[18] J.E. Mooij, B.J. van Wees, L.J. Geerligs, M. Peters, R. Fazio, and G. Schön, Phys. Rev. Lett. **65**, 645 (1990).

[19] D.R. Hofstadter, Phys. Rev. B **14**, 2239 (1976).

[20] A. Kampf and G. Schön, Phys. Rev. B **37**, 5954 (1988).

[21] P. Niyaz, R.T. Scalettar, C.Y. Fong, and G.G. Batrouni, Phys. Rev. B **44**, 7143 (1991).

[22] M.V. Feigel'man and K. Ziegler, Phys. Rev. B **46**, 6647 (1992).